

Extended Data Table 1 | Dominant ring- and diffuse-porous species at the Smithsonian Conservation Biology Institute (SCBI) and Harvard Forest, along with sample sizes included in this analysis.

	species	dendrometer bands		tree cores	
		n trees	n tree-years	n cores	date range
<b>SCBI</b>					
ring-porous	<i>Carya cordiformis</i>	0	0	18	1917-2009
	<i>Carya glabra</i>	0	0	39	1901-2009
	<i>Carya ovalis</i>	0	0	24	1896-2009
	<i>Carya tomentosa</i>	0	0	17	1926-2009
	<i>Fraxinus nigra</i>	0	0	16	1901-2016
	<i>Fraxinus americana</i>	0	0	69	1910-2009
	<i>Quercus alba</i>	34	197	66	1904-2009
	<i>Quercus montana</i>	0	0	67	1893-2009
	<i>Quercus rubra</i>	35	229	71	1870-2009
	<i>Quercus velutina</i>	0	0	83	1902-2009
diffuse-porous	<i>Fagus grandifolia</i>	13	89	81	1932-2009
	<i>Liriodendron tulipifera</i>	41	354	109	1920-2009
<b>Harvard Forest</b>					
ring-porous	<i>Fraxinus americana</i>	9	27	34	1901-2008
	<i>Quercus alba</i>	118	575	179	1901-2014
	<i>Quercus velutina</i>	11	50	0	
diffuse-porous	<i>Fagus grandifolia</i>	8	45	0	
	<i>Betula lenta</i>	8	44	0	
	<i>Betula populifolia</i>	5	24	0	
	<i>Betula papyrifera</i>	3	13	0	
	<i>Betula alleghaniensis</i>	21	90	44	1952-2013
	<i>Prunus serotina</i>	9	37	0	
	<i>Acer rubrum</i>	144	669	59	1930-2014
	<i>Acer pensylvanicum</i>	4	16	0	

Extended Data Table 2 | Summary of parameters describing the phenology and temperature sensitivity of ring- and diffuse- porous species groups at the Smithsonian Conservation Biology Institute (SCBI) and Harvard Forest.

	SCBI		Harvard Forest	
	ring-porous	diffuse-porous	ring-porous	diffuse-porous
critical $T_{max}$ window	3/22-4/9	2/19-5/21	4/2-5/7	3/19-5/7
<b>Stem Growth</b>				
$DOY_{25}$	123 (May 4)	154 (June 4)	132 (May 15)	164 (June 14)
$DOY_{50}$	152 (June 2)	172 (June 22)	159 (June 9)	182 (July 2)
$DOY_{75}$	180 (June 30)	190 (July 9)	186 (July 6)	199 (July 19)
$DOY_{g_{max}}$	152 (June 2)	173 (June 23)	161 (June 11)	183 (July 3)
$g_{max}$ (mm/day)	0.046	0.061	0.03	0.025
$L_{pgs}$	56.5	35.8	54.5	35.1
$\Delta DBH$ (mm/yr)	4.7	3.6	3.1	1.4
<b>Canopy Foliage (ecosystem level)</b>				
Greenup	101 (April 11)		115 (April 25)	
Mid-greenup	120 (April 30)		137 (May 17)	
Peak	173 (June 22)		182 (July 1)	
Senescence	215 (Aug. 3)		218 (Aug. 6)	
<b>Phenological temperature sensitivity* (days/°C)</b>				
Stem growth:				
$DOY_{25}$	1.9 ± 0.68	3.5 ± 0.81	2.8 ± 1.05	7.9 ± 1.3
$DOY_{50}$	1.5 ± 0.90	3.5 ± 1.0	5 ± 1.7	7.3 ± 1.5
$DOY_{75}$	1.1 ± 1.6	3.6 ± 1.5	7.2 ± 2.7	6.6 ± 3.1
$DOY_{g_{max}}$	1.6 ± 0.89	3.5 ± 1.0	3.3 ± 1.8	6.7 ± 1.7
Canopy foliage:				
Greenup	4.5 ± 1.15		2.4 ± 1.6	
Mid-greenup	4.07 ± 0.74		3.0 ± 0.92	
Peak	3.67 ± 1.87		0.81 ± 1.1	
Senescence	2.76 ± 2.34		1.1 ± 1.5	

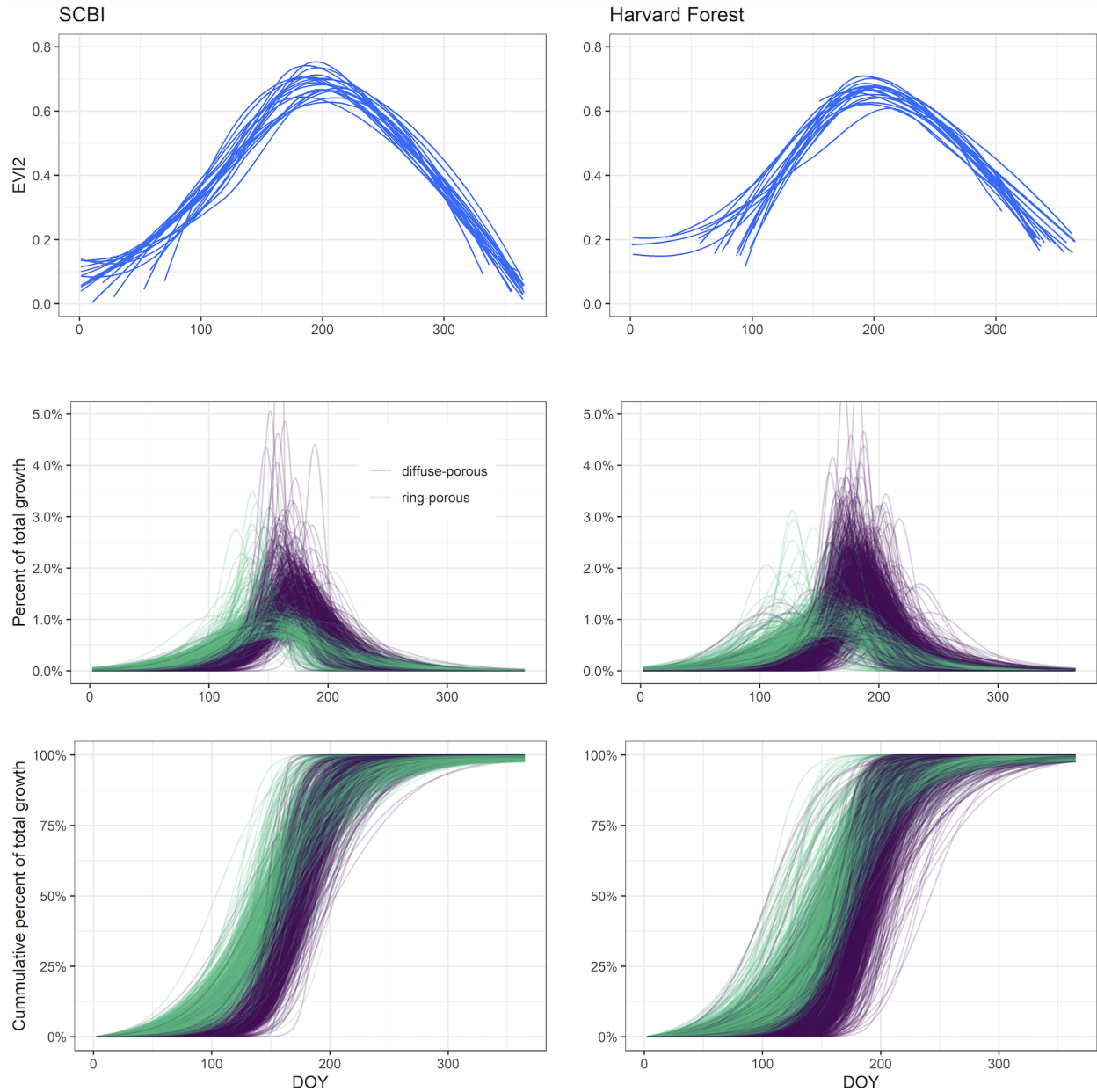
\*Phenological temperature sensitivity refers to the sensitivity of a parameter to the mean maximum temperature ( $T_{max}$ ) during the critical temperature window (Fig. 1). Because leaf phenology measurements were derived from satellite imagery and included both ring- and diffuse-porous trees, the selection of a critical window was less straightforward. We used the critical window identified for diffuse-porous trees as the critical window for leaf phenology calculations because they included a wider range of spring dates.

Extended Data Table 3 | Summary of tree-ring chronologies analyzed and number of significant (at  $p=0.05$ ) positive or negative correlations of ring width index to monthly  $T_{max}$  in univariate and multivariate analyses.

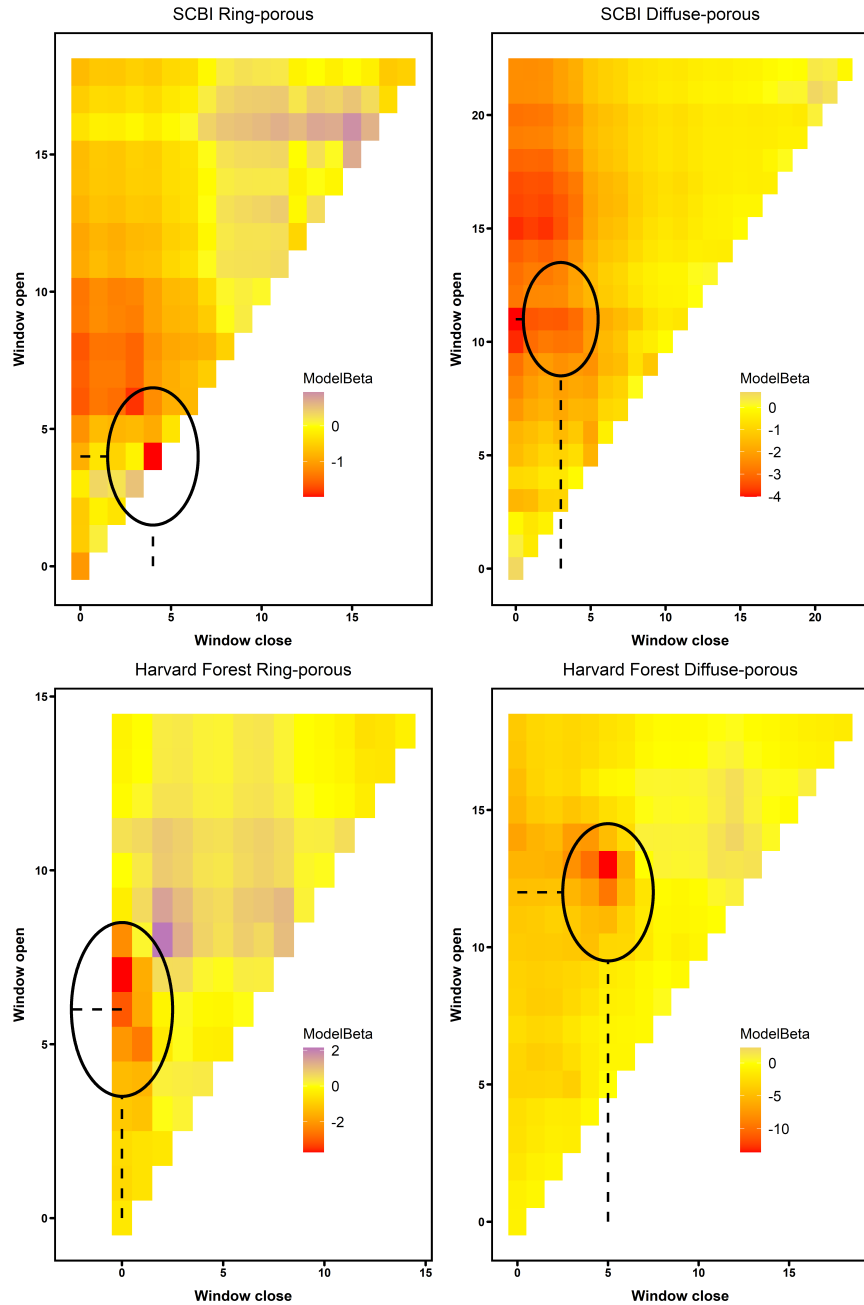
species	n	n. correlations to monthly mean max. T significant at $p=0.05$													
		univariate analysis										multivariate analysis			
		April		May		June		July		Aug		April		June-July	
<b>Ring-porous</b>															
<i>Carya cordiformis</i>	1	0	0	0	0	1	0	1	0	0	0	0	0	0	1
<i>Carya glabra</i>	7	0	0	0	0	3	0	5	0	5	0	0	0	0	5
<i>Carya ovalis</i>	1	1	0	0	1	0	0	0	0	0	1	0	0	0	0
<i>Carya ovata</i>	21	0	0	0	0	5	0	20	0	17	0	12	2	0	0
<i>Carya tomentosa</i>	2	0	0	0	0	1	0	2	0	0	0	2	0	0	1
<i>Fraxinus americana</i>	5	0	0	0	0	4	0	3	0	2	1	0	0	0	3
<i>Fraxinus nigra</i>	2	0	0	0	0	0	0	1	0	1	0	1	0	0	1
<i>Quercus alba</i>	36	0	4	0	18	0	31	0	30	0	24	0	2	0	33
<i>Quercus macrocarpa</i>	1	0	0	0	0	0	0	1	0	1	0	1	0	0	1
<i>Quercus mongolica</i>	16	0	2	1	3	0	10	0	9	0	3	1	2	0	11
<i>Quercus montana</i>	1	0	0	0	1	0	0	0	0	0	0	0	0	0	0
<i>Quercus pagoda</i>	1	0	0	0	1	0	1	0	1	0	1	0	0	0	1
<i>Quercus rubra</i>	37	0	2	1	4	0	25	0	18	1	5	1	1	0	22
<i>Quercus stellata</i>	3	0	0	0	1	0	2	0	1	0	0	0	0	0	2
<i>Quercus velutina</i>	7	0	0	0	2	0	5	0	6	0	3	0	0	0	7
<b>TOTAL</b>	<b>141</b>	<b>1</b>	<b>8</b>	<b>2</b>	<b>45</b>	<b>0</b>	<b>107</b>	<b>0</b>	<b>91</b>	<b>2</b>	<b>53</b>	<b>4</b>	<b>5</b>	<b>0</b>	<b>108</b>
<b>Diffuse-porous</b>															
<i>Acer rubrum</i>	4	0	1	0	0	0	1	0	1	0	0	0	1	0	3
<i>Acer saccharum</i>	16	1	0	0	2	0	14	0	12	0	6	3	0	0	14
<i>Betula alleghaniensis</i>	2	0	0	0	0	0	2	0	0	0	0	0	0	0	1
<i>Betula lenta</i>	3	0	0	0	1	0	1	0	1	0	0	0	0	0	2
<i>Fagus grandifolia</i>	6	1	0	0	0	0	4	0	5	0	1	1	0	0	5
<i>Liriodendron tulipifera</i>	32	2	1	0	7	0	30	0	17	0	16	1	0	0	27
<i>Magnolia acuminata</i>	1	0	0	0	0	0	0	0	0	0	0	0	0	0	0
<i>Nyssa sylvatica</i>	1	0	0	0	0	0	0	0	0	0	0	0	0	0	0
<i>Populus grandidentata</i>	1	0	0	0	0	0	0	0	0	0	0	0	0	0	0
<b>TOTAL</b>	<b>66</b>	<b>4</b>	<b>2</b>	<b>0</b>	<b>10</b>	<b>0</b>	<b>52</b>	<b>0</b>	<b>36</b>	<b>0</b>	<b>23</b>	<b>5</b>	<b>1</b>	<b>0</b>	<b>52</b>
<b>TOTAL</b>	<b>207</b>	<b>5</b>	<b>10</b>	<b>2</b>	<b>55</b>	<b>0</b>	<b>159</b>	<b>0</b>	<b>127</b>	<b>2</b>	<b>76</b>	<b>9</b>	<b>6</b>	<b>0</b>	<b>160</b>



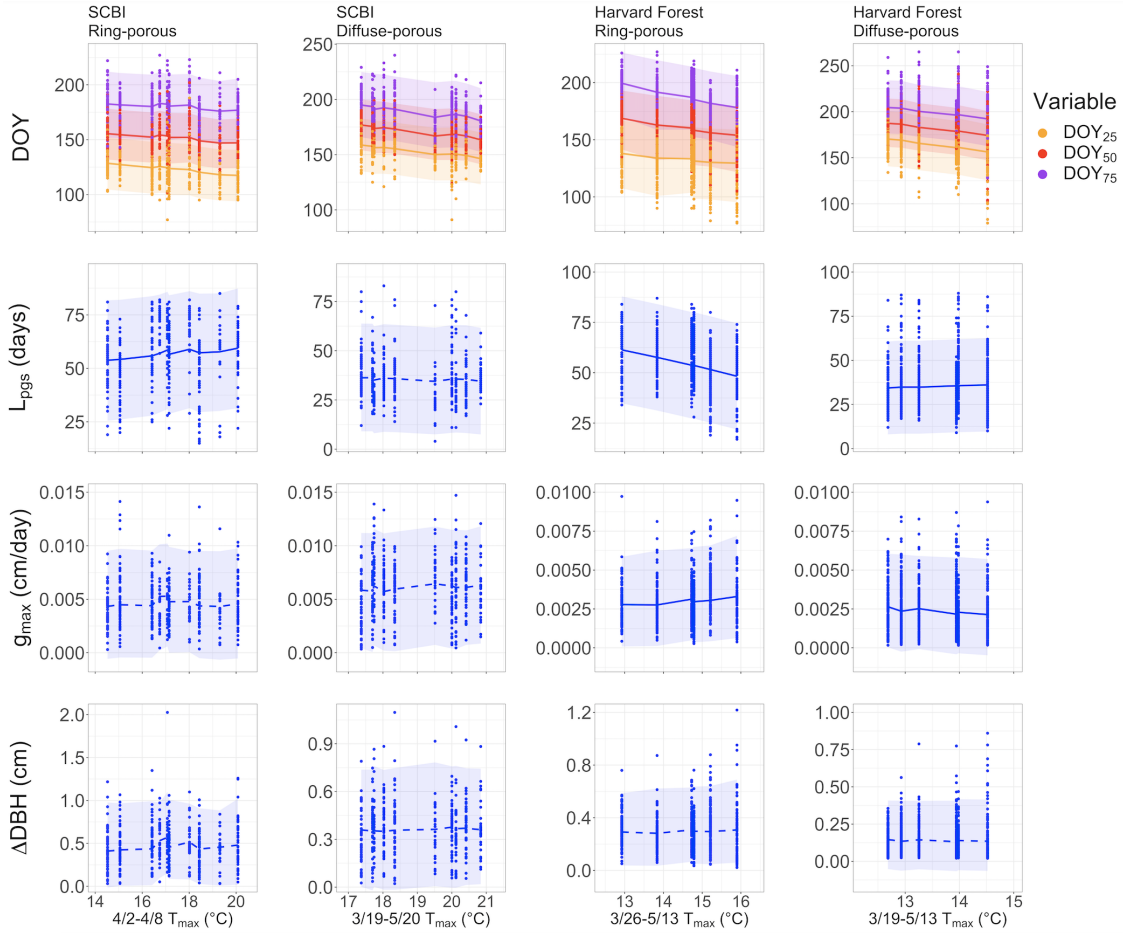
**Extended Data Figure 1 | Map of sampling locations of tree-ring chronologies analyzed in this study.** Sites are colored by the xylem porosity type of species sampled: ring porous (RP), diffuse porous (DP), or both. Sampling details are provided in SI Table 1.



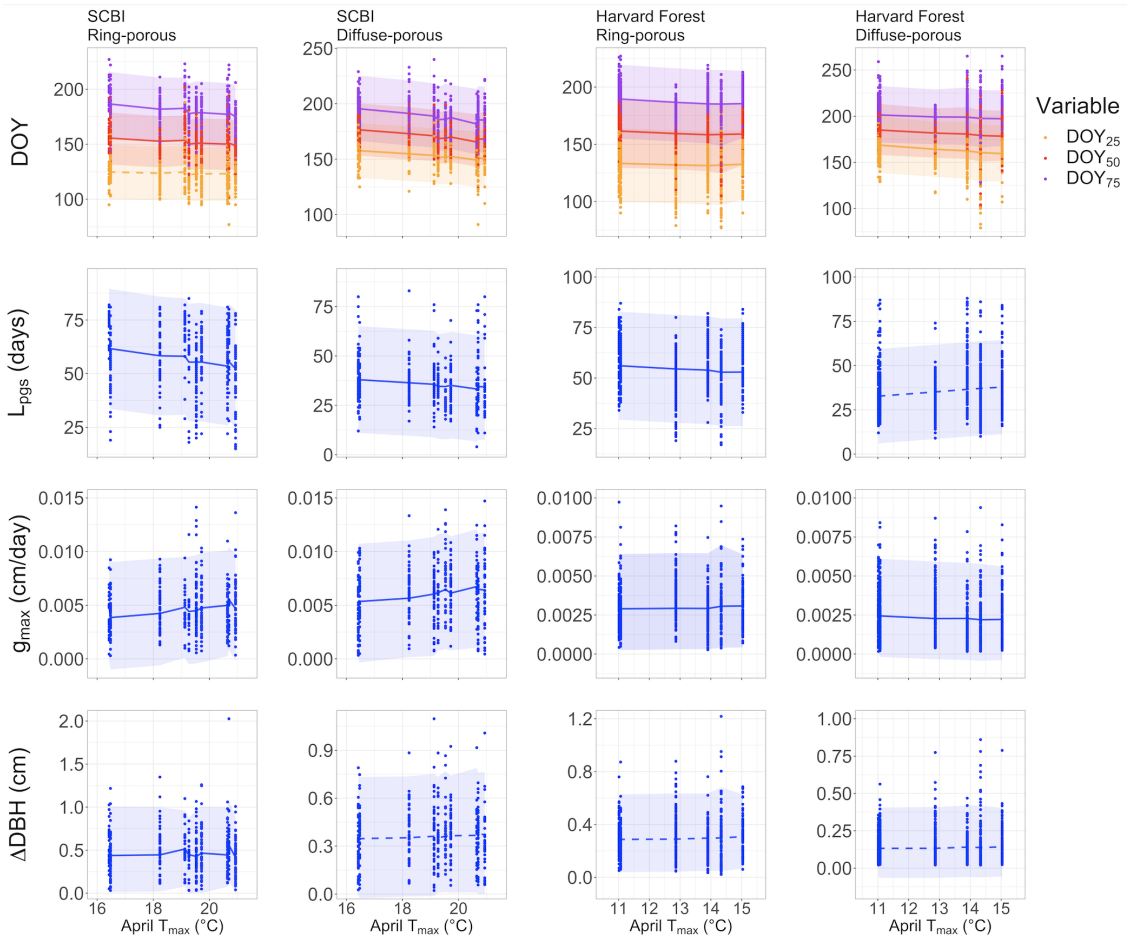
**Extended Data Figure 2 | Phenological patterns of forest canopy greenness (top row) and stem growth of ring- and diffuse-porous trees, represented as both relative and cumulative fractions of total annual growth (middle and bottom rows, respectively), at the Smithsonian Conservation Biology Institute (SCBI) and Harvard Forest.** In the top row, canopy greenness is characterized using the two band Enhanced Vegetation Index (EVI2), with each line representing a year between 2000 and 2018. For stem growth, each line represents the growth of one tree over one year, as modeled based on a five-parameter logistic growth model to dendrometer band data.



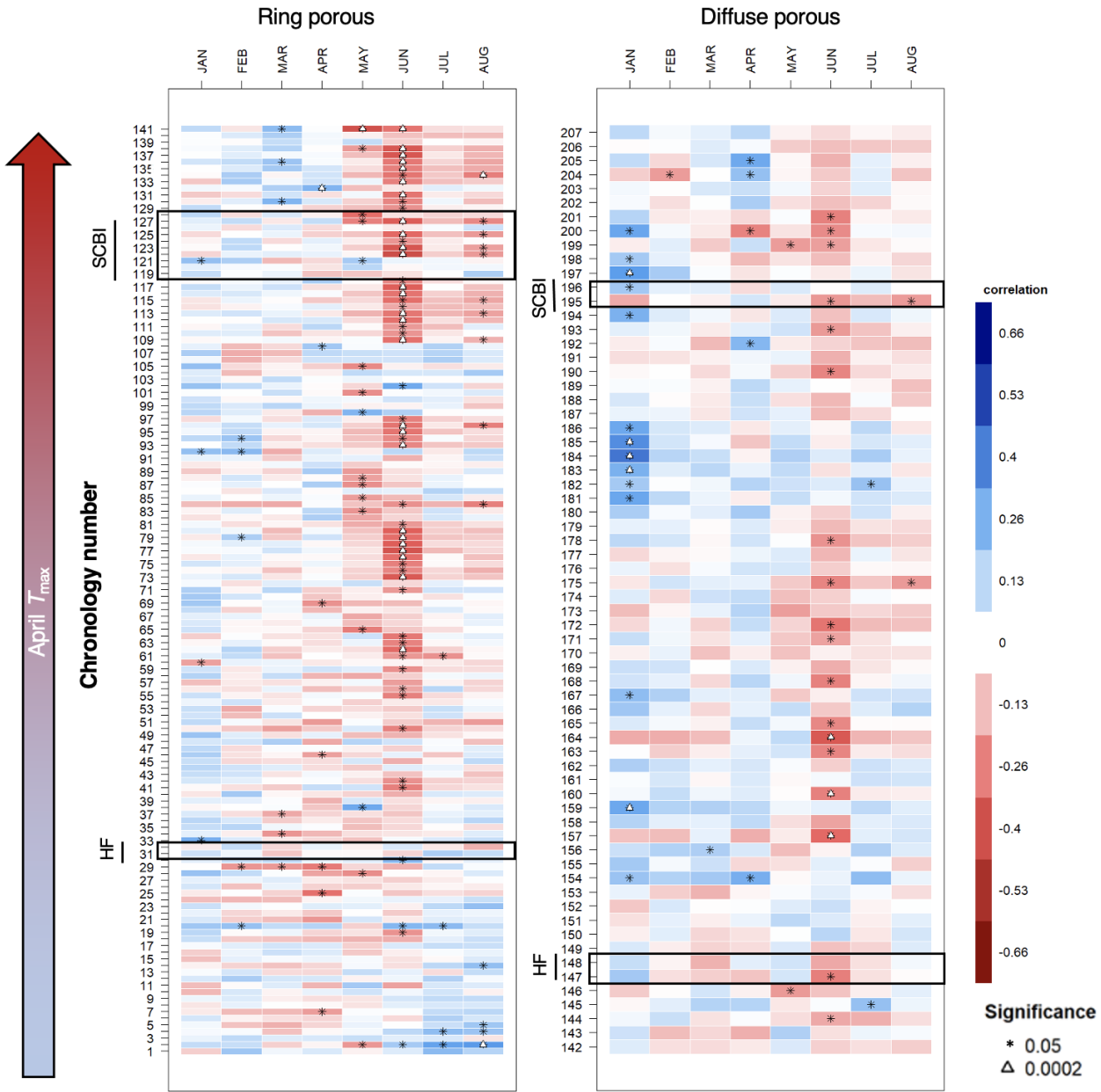
**Extended Data Figure 3 | Landscapes of relationships between the day of year on which 25% of annual growth is achieved ( $DOY_{25}$ ) and temperature in prior weeks for ring- and diffuse-porous trees at the Smithsonian Conservation Biology Institute (SCBI) and Harvard Forest.** Shown are matrices of  $\beta$  coefficients from first-order linear regressions between mean maximum temperature ( $T_{max}$ ) and  $DOY_{25}$ . Window Open and Window Close indicate number of weeks prior to  $DOY_{25}$  (listed in Extended Data Table 2). Yellow shading indicates neutral relationships, while orange or red shading indicates that  $DOY_{25}$  advances with increased  $T_{max}$  over the given time window (negative  $\beta$ ). Black circles indicate the critical temperature window selected based on minimization of  $\Delta AICc$ , the difference in Akaike Information Criterion corrected for small sample size relative to a null model. Critical temperature windows are listed in Extended Data Table 2.



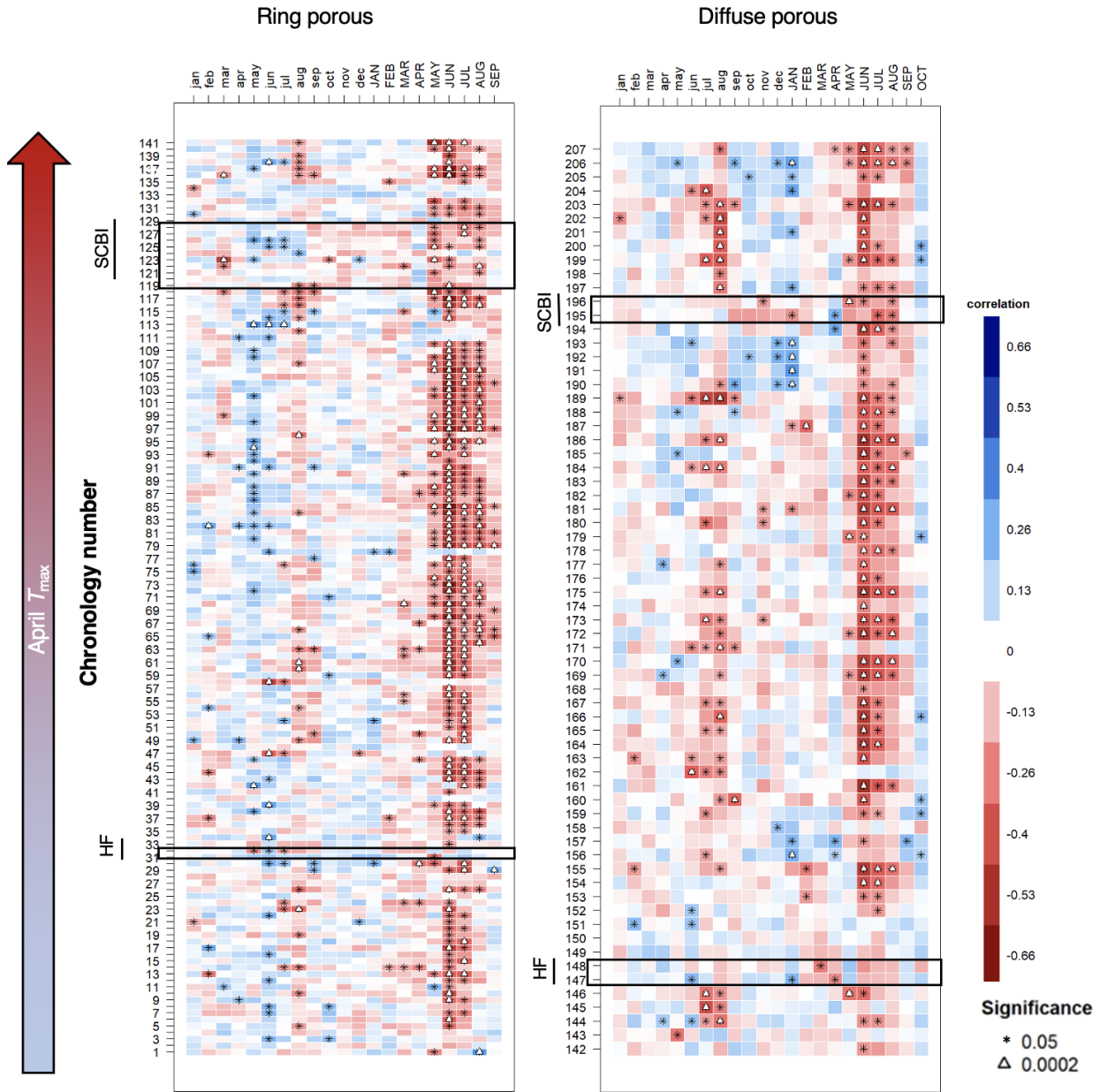
**Extended Data Figure 4 | Response of stem growth phenology and rates to mean maximum temperatures ( $T_{max}$ ) during the spring critical temperature window (CTW) for ring- and diffuse-porous species at the Smithsonian Conservation Biology Institute (SCBI) and Harvard Forest.** CTW was defined as the period over which  $T_{max}$  was most strongly correlated with the day of year on which 25% of annual growth was achieved ( $DOY_{25}$ ; Extended Data Table 2, Extended Data Figure 3). Shown are relationships between mean  $T_{max}$  over the CTW and days of the year on which 25%, 50%, and 75% total stem growth were achieved ( $DOY_{25}$ ,  $DOY_{50}$ ,  $DOY_{75}$ , respectively; first row); the length of the peak growing season ( $L_{pgs}$ ; second row); maximum growth rate ( $g_{max}$ ; third row); and total seasonal radial stem growth ( $\Delta DBH$ ; fourth row). Posterior predictions of each variable that did not include zero are represented with solid lines, while those that do include zero use dotted lines. 95% credible intervals are represented by bands. For both species groups at both sites,  $DOY_{25}$ ,  $DOY_{50}$ , and  $DOY_{75}$  all declined significantly with mean  $T_{max}$  during their respective CTW. Dots represent growth parameter values for individual tree-year combinations, which were derived by fitting a five-parameter logistic growth model to dendrometer band data.



**Extended Data Figure 5 | Response of stem growth phenology and rates to April mean maximum temperature ( $T_{max}$ ) for ring- and diffuse-porous species at the Smithsonian Conservation Biology Institute (SCBI) and Harvard Forest.** Shown are relationships between April  $T_{max}$  and days of the year on which 25%, 50%, and 75% total stem growth were achieved ( $DOY_{25}$ ,  $DOY_{50}$ ,  $DOY_{75}$ , respectively; first row); the length of the peak growing season ( $L_{pgs}$ ; second row); maximum growth rate ( $g_{max}$ ; third row); and total seasonal radial stem growth ( $\Delta DBH$ ; fourth row). Posterior predictions of each variable that did not include zero are represented with solid lines, while those that do include zero use dotted lines. 95% credible intervals are represented by bands. For both species groups at both sites,  $DOY_{25}$ ,  $DOY_{50}$ , and  $DOY_{75}$  declined significantly with April  $T_{max}$ , with the exception of  $DOY_{25}$  for ring-porous species at SCBI. Dots represent growth parameter values for individual tree-year combinations, which were derived by fitting a five-parameter logistic growth model to dendrometer band data.



**Extended Data Figure 6 | Sensitivity of annual growth, as derived from tree-rings, to monthly mean minimum temperatures ( $T_{min}$ ), for 207 chronologies from 108 sites across eastern North America** (Extended Data Figure 1). Colors indicate the correlation between monthly  $T_{min}$  and a dimensionless ring width index (RWI) derived from the multiple trees that form each chronology and emphasizing interannual variability associated with climate. Chronologies are grouped by xylem porosity and ordered by mean April  $T_{min}$ . Plots are annotated to highlight records from our two focal sites, the Smithsonian Conservation Biology Institute (SCBI) and Harvard Forest (HF) (Extended Data Table 1). Species analyzed and numbers of significant correlations to  $T_{min}$  are summarized in Extended Data Table 3, and chronology details are given in SI Table 1.



**Extended Data Figure 7 | Sensitivity of annual growth, as derived from tree-rings, to monthly mean maximum temperatures ( $T_{max}$ ) of the current and past year, for 207 chronologies from 108 sites across eastern North America** (Extended Data Figure 1). Colors indicate the correlation between monthly  $T_{max}$  and a dimensionless ring width index (RWI) derived from the multiple trees that form each chronology and emphasizing interannual variability associated with climate. Chronologies are grouped by xylem porosity and ordered by mean April  $T_{max}$ . Plots are annotated to highlight records from our two focal sites, the Smithsonian Conservation Biology Institute (SCBI) and Harvard Forest (HF) (Extended Data Table 1). Figure presents the same results as main manuscript Fig. 3 but extends back to include the previous year. Species analyzed and numbers of significant correlations to  $T_{max}$  are summarized in Extended Data Table 3, and chronology details are given in SI Table 1.